16th World Conference on Earthquake, 16WCEE 2017
Santiago Chile, January 9th to 13th 2017
Paper N° 1140
Registration Code: S-D1462223775

EXPERIMENTAL AND ANALYTICAL STUDY OF GIRDER UNSEATING IN SKEW BRIDGES DURING EARTHQUAKES

S. Wu[(1)], I. G. Buckle[(2)], A. M. Itani[(2)]

[(1)] Research Assistant, Department of Civil and Environmental Engineering, MS258, University of Nevada, Reno, Reno, NV, 89557, United States of America, seismic1989@gmail.com
[(2)] Professor, Department of Civil and Environmental Engineering, MS258, University of Nevada, Reno, Reno, NV, 89557, United States of America, igbuckle@unr.edu, itani@unr.edu

Abstract

Skew bridges are known to be more vulnerable to unseating during earthquakes than straight bridges of the same span length. Various reasons for this vulnerability have been proposed based on simplified modeling and empirical evidence and many design codes increase the minimum support length requirements for skewed bridges by factors based on engineering judgment. In this paper, an unseating mechanism is proposed based on observed unseating of skew bridges in recent earthquakes. It is hypothesized that under earthquake action, a skewed bridge superstructure first closes the expansion gap, then impacts the abutment back wall, and finally rotates about the obtuse corner, leading to excessive in-plane displacements at the acute corner at the opposite end of the span. In addition, shake table experiments of single-span simply supported skew bridges with seat-type abutments are introduced, which have recently been conducted in the Earthquake Engineering Laboratory at the University of Nevada, Reno. The objectives of the experiment were to: (1) test the proposed unseating mechanism; (2) validate a detailed 3D analytical model developed in OpenSees that considers pounding and friction effects at the abutment; and (3) confirm the applicability of the simplified method for estimating the additional support length required due to skew. Details of the design, instrumentation, and setup of the experiments are described. Impact forces between bridge deck and abutment were measured as well as the displacements, accelerations, and rotations of the superstructure. It is shown that the proposed unseating mechanism matches well with the observed behavior. The experimental results indicate that the combination of forced vibration in translational modes and free vibration in rotational mode around the center of stiffness of substructure leads to the unseating of symmetrical skew bridge at acute corners. Furthermore, a rigorous OpenSees model which accounts for the impact and sliding effects between the bridge deck and abutment was developed and details of the model are introduced. Good correlation is obtained between the experiment and the OpenSees model. The implications for revising the minimum support length requirements have yet to be studied.

Key words: skew bridges; girder unseating; shake table experiments; dynamic analysis

1. Introduction

Seat-type abutments are commonly used in bridges to avoid large, unbalanced stresses that could develop in the superstructure and embankment backfill due to temperature loading, creep, shrinkage, and prestress shortening. Seat-type abutments have a gap between the end of the bridge and the abutment backwall which is bridged by a movement joint. However, this gap is not always sized to accommodate the seismic displacement demands. During large earthquakes, the gap is forced to close, resulting in abutment pounding. Typically, this pounding effect reduces the relative displacement of superstructure in straight bridges by adding stiffness and dissipating energy. However, when it comes to skew bridges, this impact results in in-plane rotation which, in turn, amplifies the global displacement response, leading to larger support length requirement in skew bridges than in their straight counterparts [1-4]. Unseating occurs at seat-type abutments when the provided support length cannot sufficiently accommodate the relative displacements of the superstructure.

Skew bridges with seat-type abutments were observed to suffer catastrophic damage including unseating at the acute corners in the past major earthquakes [3-8], such as the Foothill Boulevard Undercrossing in the 1971 San Fernando earthquake [5] and the Mission Gothic and Gavin Canyon Undercrossings in the 1994 Northridge earthquake [6]. This is mainly due to the in-plane rotation of superstructure. Many researches have been conducted to investigate the cause of in-plane rotation. Eccentricity between the centers of mass and stiffness is taken as the most common explanation, but this rotation has also been observed in perfectly symmetrical bridges. In these cases abutment pounding followed by rotation about the vertical axis has been suggested as the unseating mechanism [1, 2, 9]. Despite the common occurrence of this type of damage, little experimental research on the interaction between the bridge deck and abutment has been conducted to validate this behavior and quantify its effect. As a consequence, explicit procedures for calculating the required support length in skew bridges are not given in current design specifications and empirical expressions based on engineering judgment are used instead. In this paper, shake table experiments of a family of single-span simply supported skewed bridges with seat-type abutments are described and the unseating mechanism of skew bridges is investigated experimentally.

In addition, this paper introduces a rigorous numerical model developed in OpenSees [10], which is then validated against the experimental results. The "BeamContact3D" element is employed to simulate impact effects. This element is based on stereo-mechanical approach that has been shown to be efficient in modeling the interaction between a bridge superstructure and abutment in horizontally curved bridges [11]. It includes the effect of impact by modifying the velocities of colliding bodies after impact based on a momentum balance and the coefficient of restitution [12, 13].

2. Proposed unseating mechanism of skew bridge during earthquakes

Based on empirical evidence from collapsed skewed bridges in recent earthquakes, an unseating mechanism is proposed, as shown in Fig. 1. Under longitudinal and transverse earthquake actions (Steps 1a, 1b), the bridge first moves towards one abutment (left abutment in Fig. 1) and impacts against the abutment back wall (Step 2). The reaction from the back wall and the transverse ground motion then turns the superstructure in a direction opposite to the skew direction (counterclockwise in Fig. 1) and the bridge rotates around the obtuse corner (Step 3). With continued rotation, the acute corners move away from the abutment and become unseated (Steps 4a, 4b).

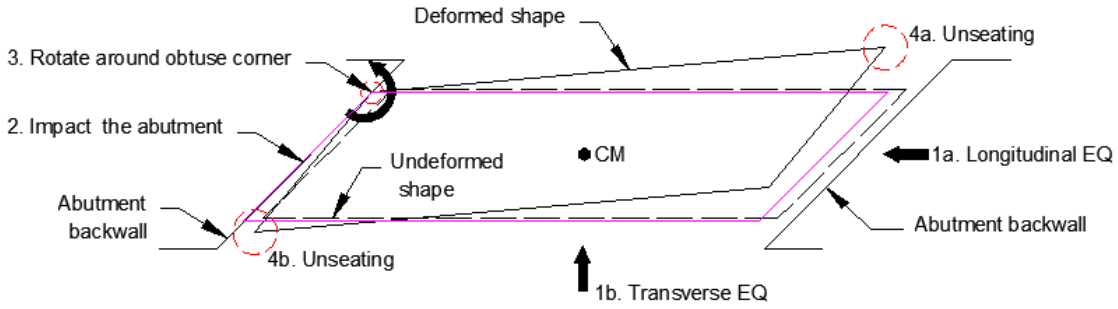

Fig. 1 – Proposed unseating mechanism of a skew bridge during earthquake action

3. Shake table experiment

In order to confirm the proposed unseating mechanism, validate the numerical model and assess the support length requirement for skew bridge, shake table experiments of a family of skew bridges were recently conducted using one of the bi-axial shake tables in the Earthquake Engineering Laboratory, University of Nevada, Reno. The details of the experiment are described in this section.

3.1 Design of bridge model

Four, single-span, simply supported bridge models with seat-type abutments were designed with skew angles of 0^0 (straight), 30^0, 45^0 and 60^0. The selection of model dimensions was driven by the shake table capacity and available space in laboratory. Given these constraints, and making allowance for the overall length of the 60^0 model (the longest of the four models to be tested), the span of the straight bridge model was taken as 10.5 ft and width 3.5 ft. Based on a span of a typical prototype bridge of 120 ft and width of 40 ft, and keeping the width constant at 3.5 ft for all the models, the scale factor for length (S_L) is calculated as:

$$S_L = 40/3.5 = 11.43 \quad (1)$$

Taking the scale factor for acceleration (S_a) equal to 1.0, the scale factor for time (S_T) is given by:

$$S_L = {S_T}^2 \quad or \quad S_T = \sqrt{S_L} = 3.381 \quad (2)$$

For the purpose of these experiments, the superstructure was assumed to be a rigid in-plane, and a 2-inch thick steel plate was selected for the superstructure. Each of the three skew superstructures consisted of a straight rectangular part and two triangular parts, as shown in Fig. 2. In order to save material, and therefore cost, the rectangular part was re-used, while the triangles were unique to the angle of skew being studied. Each triangle was connected to the rectangle by two splice plates and slip-critical bolts. The dimensions and properties of the four specimens are summarized in Table 1.

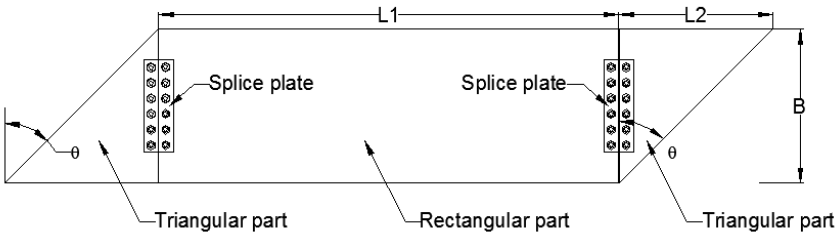

Fig. 2 – Plan view of typical single-span skew bridge model

Table 1 – Dimensions and properties of the four models

Case #	θ (°)	B (ft)	L_1 (ft)	L_2 (ft)	L (ft)	L/B	t (in)	m (kip-s^2/ft)	W (kips)
Case 1	0	3.5	10.5	0.00	10.50	3.00	2.0	0.093	3.00
Case 2	30	3.5	10.5	2.00	12.50	3.57	2.0	0.111	3.57
Case 3	45	3.5	10.5	3.50	14.00	4.00	2.0	0.124	4.00
Case 4	60	3.5	10.5	6.00	16.50	4.71	2.0	0.146	4.72

Note: L_1 is the length of the straight rectangular superstructure (Fig. 2)
L_2 is the length of the triangular part (Fig. 2)

Four elastomeric bearings were designed to support the above single-span superstructure, one at each corner, resulting in a symmetric bridge model in both geometry and stiffness. Each elastomeric bearing was circular in shape with a diameter of 3.25 in and comprised a single, 0.5 in thick, layer of rubber vulcanized to two, 0.875 in thick, end plates. The bearing dimensions were not scaled from prototype bearings by S_L, but were instead sized to give a period for the straight model of 0.21 s. This period was derived by scaling an assumed prototype period of 0.7 s by S_T.

It is noted that this model satisfies the similitude requirements for displacement and acceleration but not for force. The measured impact forces cannot therefore be scaled to obtain prototype impact forces. To be able to do so requires the attachment of significant additional mass to the model superstructure, which in turn would require increasing the stiffness of the bearings to maintain the period at 0.21 s. It was decided not to add mass

since the main focus of this study is the unseating of skew decks which is displacement driven. Prototype impact forces can be found using validated numerical models such as the one described in Sec. 4.

The abutment consisted of a face beam and a steel angle-section back wall as shown in Fig. 3(a). The face beam and back wall were W4×13 and L8×6×3/4 respectively. The long leg of the angle section was oriented in the vertical direction to accommodate the installation of $6\frac{1}{16}\ in$ diameter axial load cells.

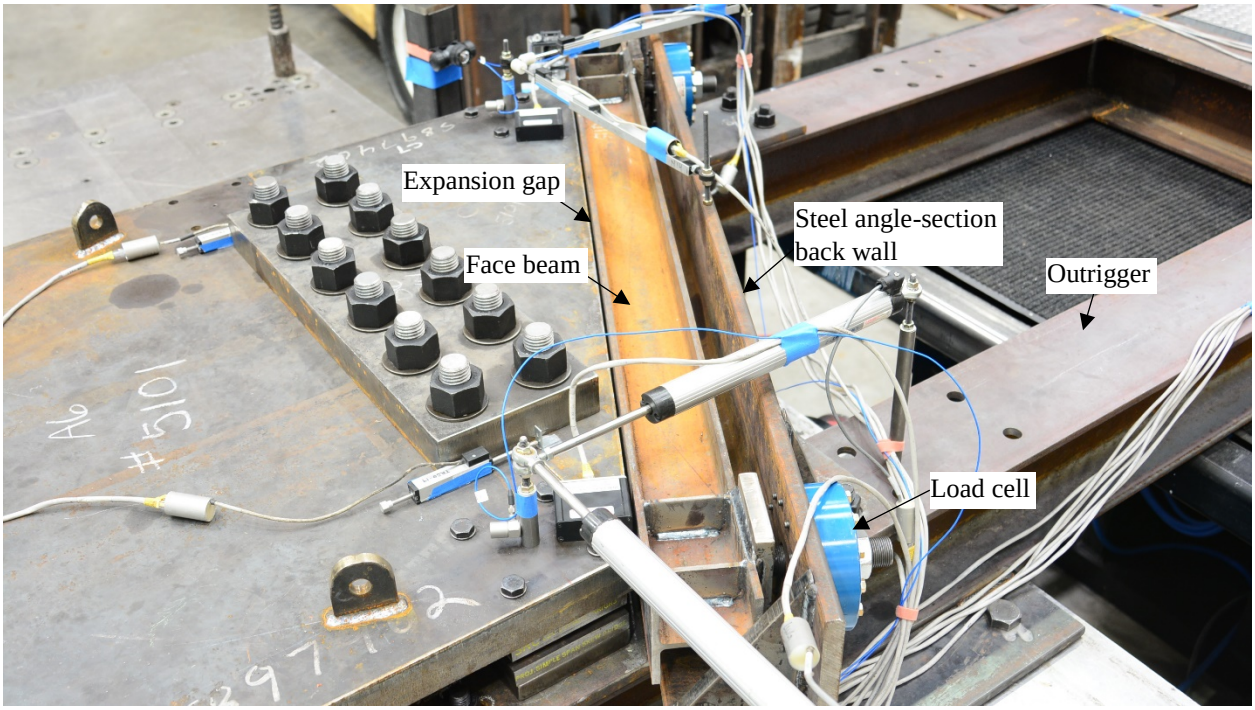

(a) Face beam is connected to abutment back wall through load cells and back wall is bolted to outrigger

(b) Side view of abutment superstructure and bearing

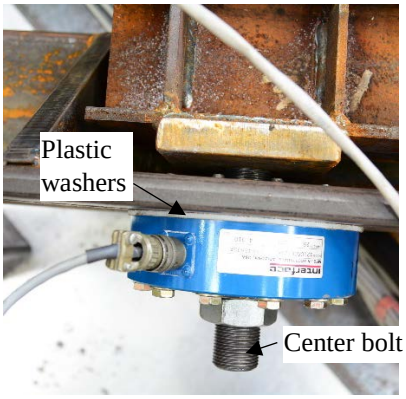

(c) Top view of load cell connection

(d) Back view of load cell

Fig. 3 –Abutment of 30º skew bridge model

The face beam was designed to provide a realistic contact surface for monitoring the impact between the abutment and superstructure. This design for the abutments had two advantages: 1) the load cells installed in the back wall measured the impact forces directly, which could then be used to calibrate numerical models and confirm the distribution of impact force along the abutment; and 2) the size of the expansion joint between the bridge deck and abutment can be easily adjusted by unbolting and rotating the load cells. The center bolt of the load cell was 1-1/4”-12UNF and 12 bolts of 5/16 in diameter were distributed around the perimeter with a

separation of 30º. Therefore, the gap size could be adjusted in increments of 30º, which corresponds to a $\Delta = 1/12/12 \approx 0.007\ in$. It follows that to make an adjustment in the gap size of 1/16 in the load cells need to be rotated through 270º. For these experiments, five gap values of 0, 1/16, 1/8, 3/16, and 1/4 in were chosen to study the effects of gap size on the superstructure response. A side view of the abutment, superstructure and bearing is also shown in Fig. 3(b).

Since the size of each biaxial shake table in the UNR Earthquake Engineering Laboratory is 14.5ft×14 ft, and the total length of the model superstructure for 60º skew (calculated from Table 1) is 22.5 ft, an outrigger is required to support the model on the table. To match the bolt holes in the table platen and the available space between two biaxial shake tables, the outrigger consisted of a grillage of two, 25.5 ft long, W8×35 beams arranged in parallel, 3ft apart, and four, W8×35 transverse diaphragms welded to the longitudinal beams, as shown in Fig. 3(a). Fig.4 shows the 45º model on Shake Table No.1 in the Earthquake Engineering Laboratory.

Fig. 4 –45º skew bridge model on Shake Table No.1

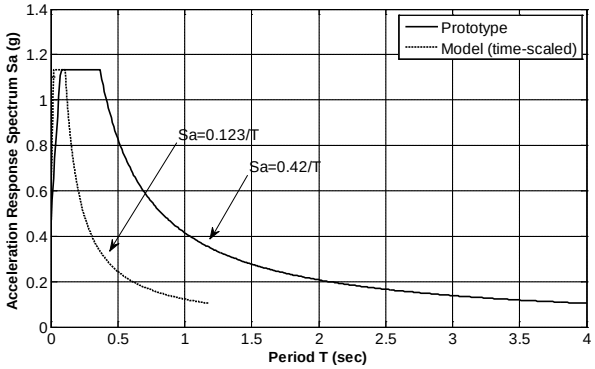

Fig. 5 – Response spectra for design-basis earthquake with 5% damping ratio

3.2 Selection of ground motion

The design-basis earthquake for the experiment assumed a rock site (AASHTO Site Class B) in AASHTO Seismic Zone 3 with a peak ground acceleration (PGA) of 0.471 g. The short-period spectral acceleration (S_s) for the site is 1.135g, and the long-period acceleration (S_1) is 0.42 g. For Site Class B, the site factors for PGA (F_{pga}), S_s (F_a) and S_1 (F_v) are equal to 1.0 and thus S_{DS} and S_{D1} are equal to 1.135g and 0.42g, respectively. For a model with a length scale factor, S_L= 11.43, the period axis of the response spectrum for the prototype is scaled by $\sqrt{S_L} = 3.381$ to obtain the spectrum for the model. Note that the scale factor for the acceleration axis is 1.0. The response spectra for the prototype and models are plotted in Fig. 5.

Three historical ground motions from PEER strong motion database [14] were selected as the input excitations to the models: 1) El Centro record, 1940 Imperial Valley Earthquake, 2) Sylmar record and 3) Century City record, 1994 Northridge Earthquake. The design levels (hereafter referred to as DE) of the above ground motions were determined by scaling the amplitude of the major component so that its spectral acceleration at 1.0 second is equal to the 1-second spectral acceleration of the design spectrum of prototype bridges (Fig. 4). The scale factors to achieve the design level of earthquake for the El Centro record, the Sylmar record and the Century City record were 0.878, 0.475 and 0.975 respectively and were applied to both the major and minor components. The input ground motions in the experiments were time scaled by $\sqrt{S_L} = 3.381$ to maintain the similitude rule in Eq. (2).

3.3 Design of instrumentation

Instrumentation was provided to measure impact forces between the bridge deck and abutment as well as displacements and accelerations of the superstructure. Novotechniks LWG225 and/or TR series with extenders were placed at each corner of the superstructure to measure relative displacements in the longitudinal and transverse directions. Three types of accelerometers with different ranges were installed on the model. Impact

accelerations normal to the abutment were measured by Kistler accelerometers with a range of ±50g, one at each corner, and acceleration parallel to the abutments by the MEM accelerometers with a range of ±16g. One tri-axial PCB accelerometer with a range of ±10,000g was installed at the center of the deck to measure the accelerations at center of mass in both longitudinal and transverse directions. Four Interface Model 1220 load cells, with capacity of ±25 kips, were installed in the abutments to measure the impact forces between the superstructure and abutment, one at each corner. Fig. 6 shows the plan view of typical instrumentation for each model.

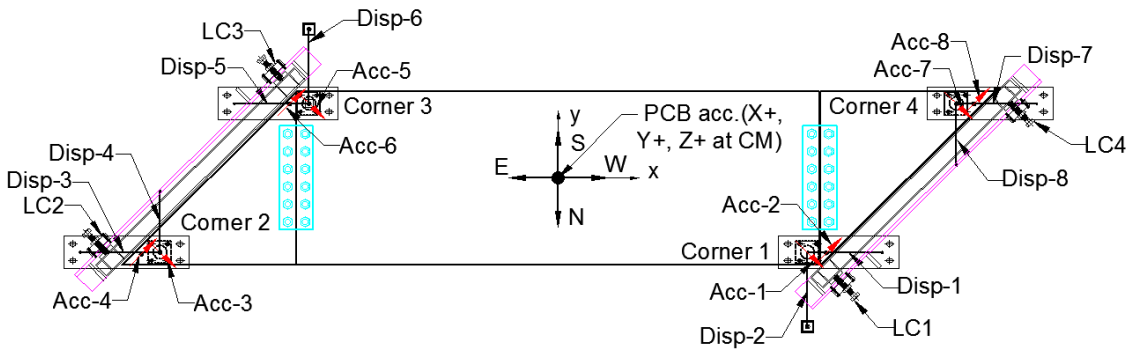

Fig. 6 – Plan view of instrumentation for 45º skew model (other models similar)

3.4 Testing protocol

The experiments began with the straight model and then moved on to the 30º, 45º, and 60º skew models. For each model, testing started with no gap at the abutment (0 in gap), and ended with a 1/4 in gap, in increments of 1/16 in. For each gap size, and each earthquake, the models were excited by: 1) the major component applied in the transverse direction only, 2) minor component in the longitudinal direction only, and 3) biaxial components in both directions. For each earthquake, the intensity was increased in five steps: 50%, 75%, 100%, 150% and 200% of the Design Earthquake (DE). It is noted that some runs were terminated earlier for reasons of safety or protection of the shake tables and/or ancillary equipment. Test parameters selected for each experiment are summarized in Table 2.

Table 2 – Summary of test parameters for the experiments

Skew, θ	0º, 30º, 45º, 60º
Abutment gap	0", 1/16", 1/8", 3/16", 1/4"
EQ record	El Centro (1940), Century City (1994), Sylmar (1994)
Scale factors	50%DE, 75%DE, 100%DE, 150%DE, 200%DE,
EQ input direction	Transverse only, Longitudinal only, Biaxial
Total runs	876

3.5 Estimation of bearing properties

In order to check the initial and final properties of the elastomeric bearings (before and after the experiments), two groups of snap tests were conducted in the transverse direction: one on the straight model before the experiment began (snap test I), and the other on the 60º skew model after the experiments were completed (snap test II). In the snap tests, the shake table was ‘snapped’ or ‘quick-released’ from an initial position to an offset position to excite the bridge deck in free vibration. Various offsets were used to exercise the bearings at higher

amplitudes. The resulting history of deck displacement was used to back-calculate the effective stiffness and damping properties. However, since the release time of the table was not instantaneous, classic free vibration was not achieved and a response history analysis was required using presumed bearing properties and the actual measured table motion. The best fit for the numerical response to experimental data gave the bearing properties. By comparing the properties at different shear strain levels for the two groups of snap tests, the properties of the elastomeric bearings were taken to be those at 50% shear strain. The equivalent stiffness at this strain was found to be unchanged before and after the experiments, and equal to 1.55kip/in, and the equivalent damping ratio was found to be 9.95%, 8.83%, 8.40%, and 7.83% for models with 0º, 30º, 45º, and 60º skew respectively. The reason for the reduction in this ratio, even though the same bearings were used for all the models, is that the mass of the models increases with skew, and therefore the value of the critical damping coefficient increases with skew.

3.6 Investigation of the unseating mechanism based on experimental observations

The unseating mechanism of skew bridges under earthquake action is investigated in this section using observations from the experiments. Displacements measured during Run 105 of the 60º skew model are used to illustrate this mechanism. In this Run, the model had 1/8" gap, and was excited by the 200% DE Sylmar record. Fig.7 shows two displaced shapes from this Run: first, at the time of impact in the lower right obtuse corner, just before maximum displacement normal to the abutment (hereafter referred to normal displacement or N) occurs at the lower left acute corner, and second at the time of occurrence of maximum N at the lower left acute corner.

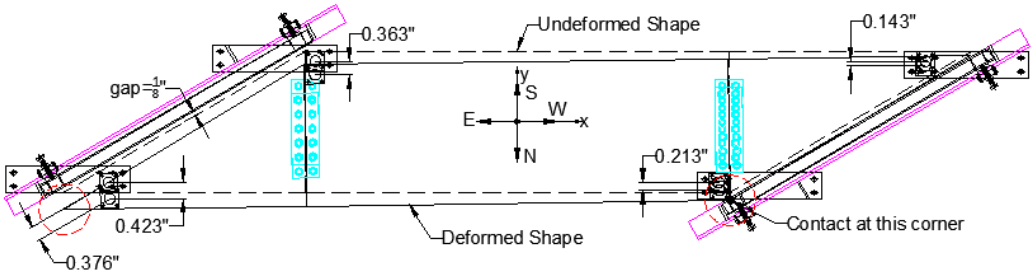

(a) At time of impact just before max. N (t = 8.1594s)

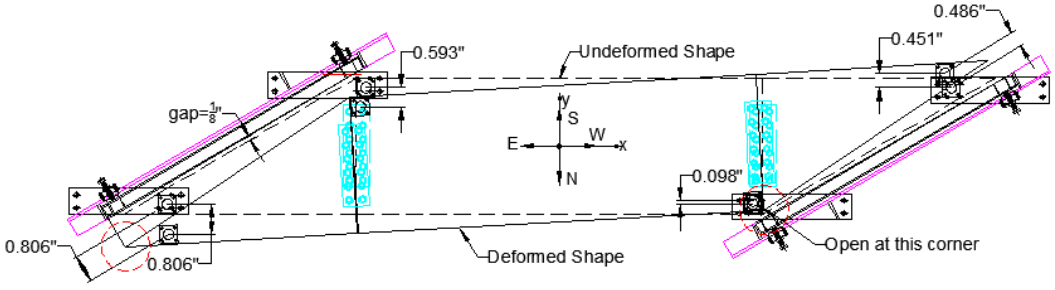

(b) At time of occurrence of max. N (t = 8.1932s)

Fig. 7 – Displaced shape of the 60º skew model at two times during Run 105

As shown in Fig. 7, the bridge deck impacted and rotated around the lower right obtuse corner, leading to the opening of the gap at the lower left acute corner. This observation matches well with proposed mechanism in Fig. 1. However, the maximum N at the lower left acute corner occurred after the impact at the lower right corner and in fact while the gap at this corner was opening as the superstructure rebounded off the face beam. Although not presented for brevity, this observation was made in all of the skew models where the earthquake motion was strong enough to close the gap and cause impact. This observation confirms the basic mechanism described in Sec. 2, but implies even larger values for N than given in Sec. 2 due to continued rotation of the

superstructure as it moves away from the point of impact. During this phase of the motion, the bridge model is rotating about the center stiffness of bearing system, which coincides with the center mass of this symmetrical model. Therefore, after the impact, the symmetrical bridge model undergoes free vibration in a rotational mode around its center stiffness, since the translational motions from the ongoing earthquake do not excite the rotational mode. It may be concluded the maximum support length demand of a symmetrical skew bridge is caused by a combination of forced vibration in translational modes and free vibration in rotational mode around the center stiffness of its substructure.

Based on the above observations, a modified unseating mechanism for skew bridges is proposed in Fig. 8. **Step 1.** The bridge deck moves laterally to close the expansion gap and impact the abutment at one end of the bridge under biaxial motions (States 1 to 2). **Step 2.** The deck rotates about the obtuse corner (State 3). **Step 3.** The deck rebounds away from the abutment and continues to rotate in same direction but now it is about the center of stiffness of substructure. This additional rotation increases the normal displacement N_{s1} and the likelihood for unseating at the adjacent acute corner (State 4). **Step 4.** If unseating does not occur at this time, then under reversed ground motion and rotation of superstructure, the bridge deck might impact at either (a) the adjacent acute corner (State 5-1), or (b) uniformly along the other abutment (State 5-2), or (c) at the other obtuse corner (State 5-3). **Step 5.** The bridge deck moves away from the abutment and rotates about the center stiffness of substructure and leads to the normal displacement N_{s2} and possible unseating at the other acute corner (State 6). The maximum support length demand of a skew bridge during earthquake action is the larger of N_{s1} and N_{s2}.

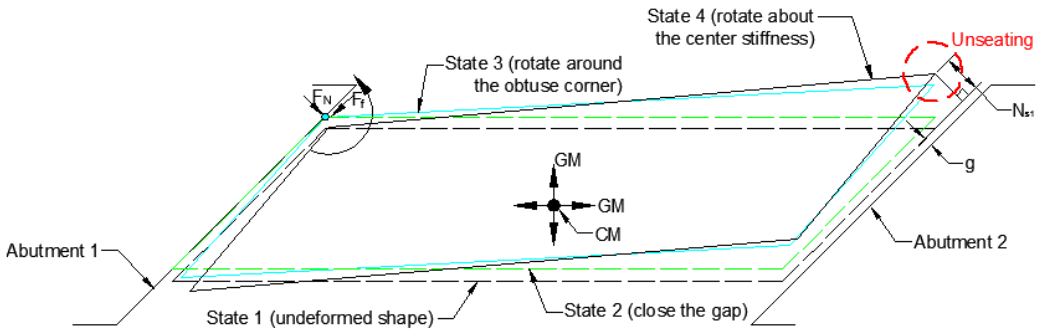

(a) States 1 to 4

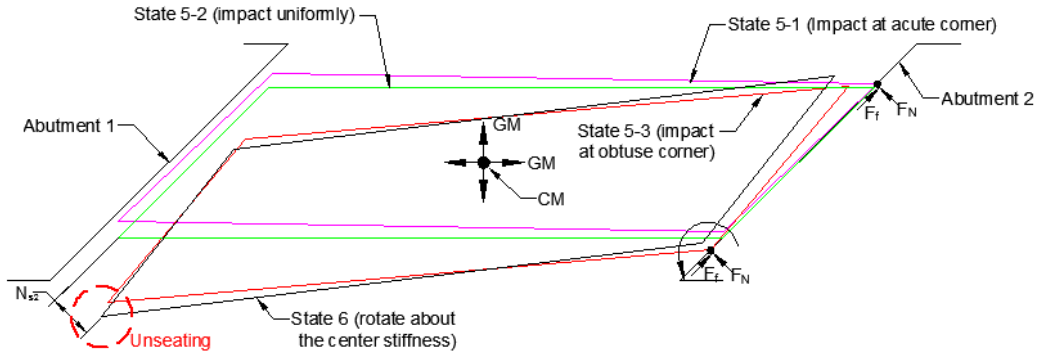

(b) States 5 to 6

Fig. 8 –Modified unseating mechanism of a skew bridge during earthquake action

4. Calibration of the numerical model in OpenSees

A three-dimensional model, including bridge-abutment interaction, was developed in OpenSees to simulate the above observed behavior. Comparison of the numerical solutions against the experimental results was used to

calibrate the numerical model. Response quantities included normal displacements at the acute corners, in-plane rotation of bridge deck, and impact forces between the deck and abutment.

In OpenSees, the superstructure was modeled by shell elements, which correctly simulated the in-plane stiffness and distributed nature of the mass. The elastomeric bearings were modeled by "zeroLength" elements with equivalent linear materials using the properties from the snap tests described in Sec. 3.5. The face beam and angle-section steel back wall were explicitly modeled by "elasticBeamColumn" elements using actual section properties. The "BeamContact3D" elements were employed to simulate the contact between the bridge deck and face beam. This element can model the gap, pounding and sliding between the deck and abutment. Impact effects are modeled by stereo-mechanical method with a coefficient of restitution equal to 1. Additional Lagrange multiplier nodes were used to enforce the contact. Friction was simulated using Coulomb's law. In the absence of test data for the coefficient of friction, a value of 0.3 for steel-on-steel was used as recommended by AISC [15]. The connection between the face beam and the angle-steel section was modeled by "twoNodeLink" element with linear materials. The constraint at the back wall of the angle-steel section was modeled by "zeroLength" element with linear materials. Rayleigh damping was used based on data from the snap tests. The numerical model for the 45º skew bridge is shown in Fig. 9.

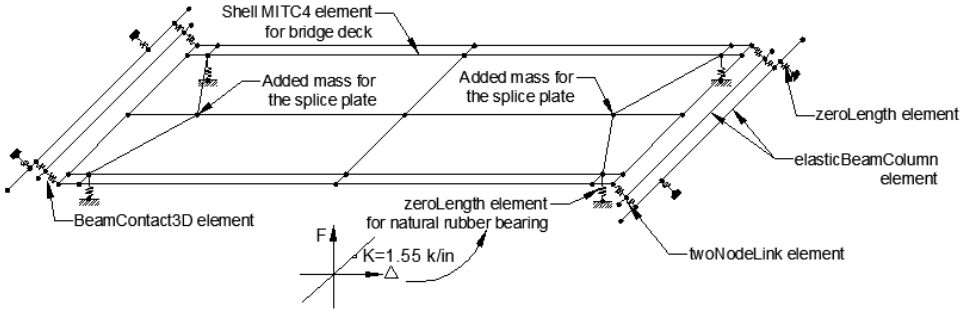

Fig. 9 –Numerical model for 45º skew bridge in OpenSees (other bridge models similar)

The numerical model was calibrated against the experimental results. Due to the space constraints, only the results for Run 125 of the 45º skew model are presented. For Run 125, the bridge model had a gap = 1/8" and was excited by 200% of the biaxial components of the scaled El Centro ground motion with the major component in transverse direction and minor component in longitudinal direction. (As noted in Sec. 3.2, this scaled motion is equal to 0.878 of the recorded El Centro ground motion.) Dynamic response analysis was performed using the achieved table motions as the input motions. As the maximum normal displacement demand of a skew bridge always occurs at the acute corners (Fig. 8), the normal displacement response histories at the acute corners are compared in Fig. 10, as well as the in-plane rotation of the deck and the total impact forces at both abutments.

Note that the locations of the corners, and the east and west abutments referenced in Fig. 10 are shown in Fig. 6. As seen in Fig.10 (a), good agreement in magnitude and phase was obtained for the normal displacements at the acute corners. Slight differences may be explained as follows:

(i) The "BeamContact3D" element in the numerical model, used a coefficient of restitution equal to 1.0, and did not consider energy dissipation due to the normal impact. This might lead to the overestimation of N.

(ii) Values for the damping ratio and stiffness of the elastomeric bearings were taken from the snap tests at 50% shear strain, whereas the actual strain varied during each earthquake run from near zero to more than 100%.

(iii) The friction coefficient between the deck and face beam in the numerical model was kept constant at 0.3, whereas in practice it will have varied due to different surface conditions along the face beam, which had not been polished prior to the experiment.

(iv) Slight variations in the size of the gap occurred across the width of the deck at each abutment, which were not included in the numerical model. This may have led to some additional rotation of the deck but the effect is considered small.

As shown in Fig. 10(b), in-plane rotation of the superstructure occurred for this symmetric, skewed bridge in both the numerical and experimental results. In the early stages of the ground motion, the time of occurrence of this rotation (phasing) in the numerical model agrees well with that in the experiment, but the magnitude is underestimated. The main reason for this observation is believed to be the use of a constant damping ratio in the numerical model (based on data for 50% shear strain) which is larger than the actual value in the experiment where the maximum shear strains exceeded 50%. Difference in phasing was also observed after several impacts, probably due to the same reason.

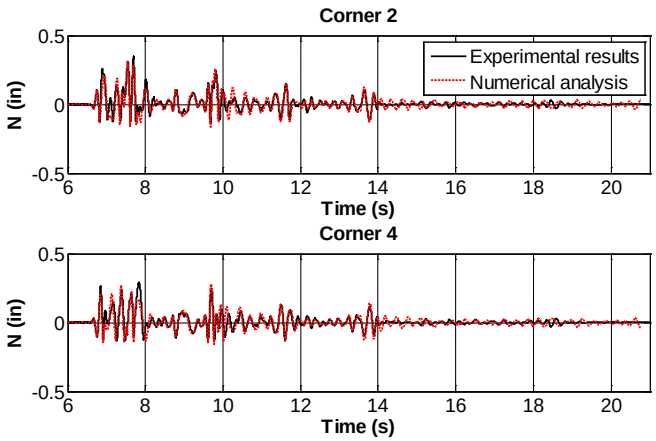

(a) Displacement N at acute corner

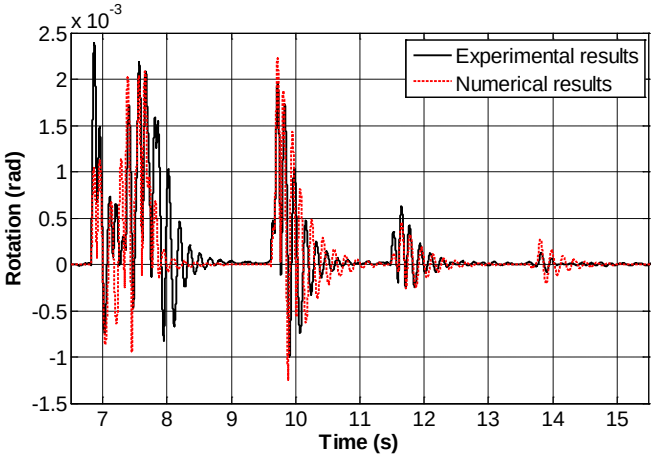

(b) In-plane rotation of superstructure

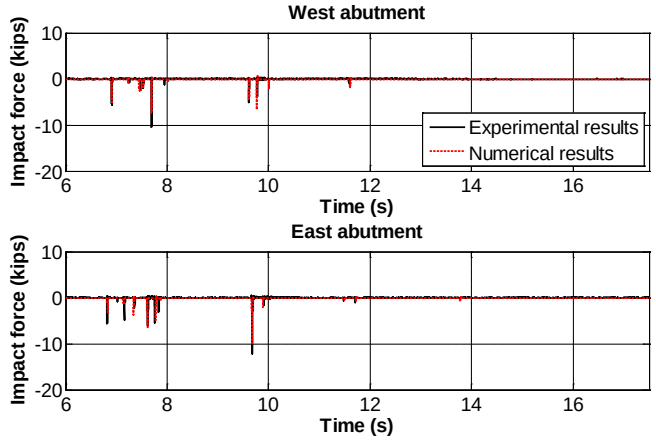

(c) Impact forces at abutments from 6.0 to 18.0 s

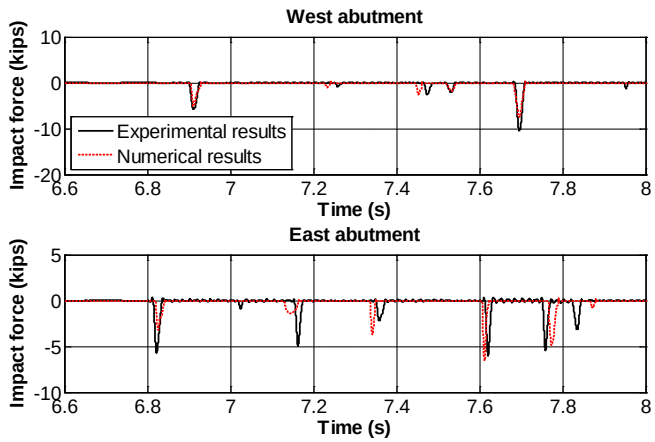

(d) Impact forces at abutments from 6.6 to 8.0 s

Fig. 10 – Comparison between numerical and experimental results for Run 125 of 45º skew model

It can be clearly seen in Fig. 10(c) that the contact between deck and abutment resulted in large impact forces of short duration. Response histories for total impact force at both abutments from the analytical analyses are in good agreement with those from the experiment for both magnitude and phase. Slight differences may be due to the same reasons listed above for the discrepancies in the normal displacements.

Similar observations were made for the response histories of the above quantities for the other Runs. Another way to show the agreement between the numerical and experimental results is to compare maximum values rather than response histories. Fig. 11 shows this comparison for maximum normal displacement (the

largest among four corners), maximum in-plane rotation, and maximum total impact force at the east and west abutments for the 45º model.

As shown in Fig. 11(a), the maximum value for N is closely estimated by the numerical model since all points fall close to the line y = x. In most cases, differences are within 20%, which is acceptable. The same observations can also be made about the maximum impact forces at the east and west abutments (Fig. 11(c) and (d)). However, as seen in Fig. 11(b), the maximum in-plane rotation is underestimated by the numerical model when the rotation is large. This may also be due to the use of stiffness and damping ratios based on test data at 50% shear strain for the elastomeric bearings when actual values for shear strain range from near zero to 160%. It is noted that similar observations were seen in the results for the other skewed models.

Based on the above results, it can be concluded that the numerical model developed in OpenSees can be used with confidence to estimate the seismic response of skew bridges. It may also be used for parameter studies on prototype bridges to evaluate the adequacy of minimum support length requirements given by AASHTO Specifications (2011) [16].

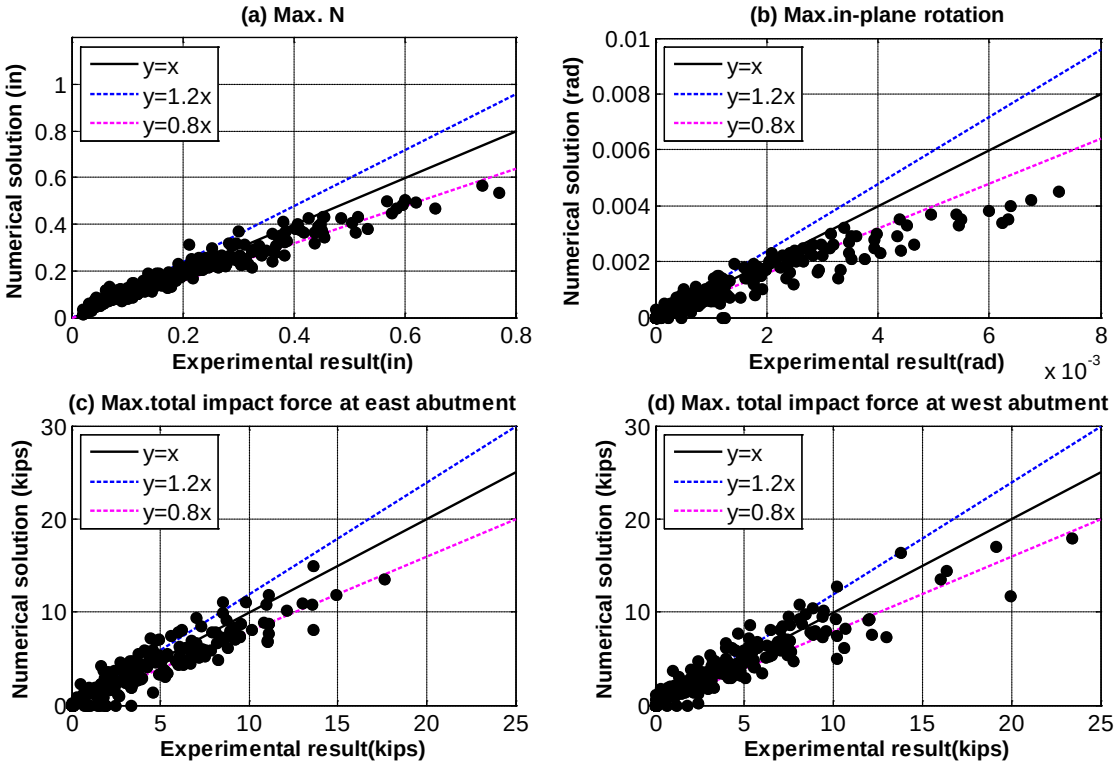

Fig. 10 – Maximum responses from numerical and experimental results for all runs on 45º skew model

5. Summary and Conclusions

An unseating mechanism in skew bridges based on superstructure impact at the abutment and followed by rotation about an obtuse corner, has been proposed based on the empirical evidence. Shake table experiments of skew bridges were conducted to verify the proposed mechanism and to investigate the seismic behavior of skew bridges. A rigorous numerical model which could account for pounding and sliding between bridge and abutments was developed and calibrated using the experimental results. It is concluded:

1. That the proposed unseating mechanism correctly depicts the behavior of a skew bridge. If the earthquake is strong enough to close the expansion gap at the abutment, the bridge impacts the abutment and rotates around the obtuse corner. Large displacements may occur at the acute corner at the opposite end of the span, but the maximum support length demand may not, however, occur until later in the motion.

2. That the maximum support length demand of a symmetrical skew bridge is caused by a combination of forced vibration in translational modes and free vibration in a rotational mode about the center stiffness of its substructure initiated by impact at the abutments.

3. That the numerical model developed for OpenSees can be used with confidence to estimate the seismic response of skew bridges. It may also be used for parameter studies on prototype bridges to evaluate the adequacy of the minimum support length requirements for skew bridges given by AASHTO [15].

Acknowledgement

Acknowledgment is made of the financial support provided by the Federal Highway Administration under Contract No. DTFH61-07-C-00031, and the expert guidance of Dr Wen-huei (Phillip) Yen (COR) and Mr. Fred Faridazar (COR) and Ms. Sheila Duwadi (COR).

References

[1] Maragakis EA (1985): A model for the rigid body motions of skew bridges. *Doctoral Thesis, Report No. EERL 85-02*, Caltech, Pasadena CA.

[2] Bjornsson, S (1997): Seismic behavior of skew bridges. *Doctoral Thesis*, University of Washington, Seattle, WA.

[3] Kawashima K, Unjoh S, Hoshikuma J I, et al (2011): Damage of bridges due to the 2010 Maule Chile Earthquake. *Journal of Earthquake Engineering*, **15**(7): 1036-1068.

[4] Buckle IG Hube M, Chen G, Yen W-H, and Arias J (2012): Structural performance of bridges in the offshore Maule Earthquake of 27 February, 2010. *Earthquake Spectra, Earthquake Engineering Research Institute*, 28, S1, s533-s552.

[5] Jennings PC, Housner GW, Hudson DE, Trifunac MD, Frazier GA, Wood JH et al (1971): Engineering features of the San Fernando earthquake of February 9, 1971. *Report no. EERL 71-02*. Pasadena (CA).

[6] Buckle IG (1994). The Northridge California earthquake of January 17, 1994: performance of highway bridges. *Report no. NCEER-94-0008*. Buffalo, New York.

[7] Kawashima K (2012): Damage of bridges due to the 2011 Great East Japan Earthquake, *Proc. Intl Symp. Engineering Lessons Learned from 2011 Great East Japan Earthquake*, Tokyo, Japan, 82–101.

[8] Chen L (2012): Report on Highway Damage in the Wenchuan Earthquake. China Communication Press.

[9] Shamsabadi, A (2007): Three-dimensional nonlinear seismic soil-abutment-foundation-structure interaction analysis of skewed bridges. *Doctoral Thesis*, University of Southern California, LA, CA, USA.

[10] McKenna F, Fenves G, and Scott M (2016). OpenSees: Open system for earthquake engineering simulation Pacific Earthquake Engineering Center, Berkeley, CA. http://opensees. berkeley.edu.

[11] Wieser J (2014): Experimental and analytical investigation of seismic bridge-abutment interaction in a curved highway bridge. *Doctoral Thesis*, University of Nevada, Reno, Reno, NV, USA.

[12] Papadrakakis M, Mouzakis H, Plevris N, Bitzarakis S (1991): Lagrange multiplier solution method for pounding of buildings during earthquakes. *Earthquake Engineering and Structural Dynamics*, 20(11): 981-998.

[13] Malhotra PK (1998): Dynamics of seismic pounding at expansion joints of concrete bridges. *ASCE Journal of Engineering Mechanics*, 124(7): 794-802.

[14] PEER NGA Database. Retrieved from http://peer.berkeley.edu/nga/

[15] AISC (2011): Steel construction manual. American institute of steel construction, 14th edition.

[16] AASHTO (2011) Guide specifications for LRFD seismic bridge design, 2nd edition. *American Association of State Highway and Transportation Officials*, Washington, DC.